Eur. Phys. J. B **61**, 405–411 (2008)
DOI: 10.1140/epjb/e2008-00108-y

THE EUROPEAN PHYSICAL JOURNAL B

Coulomb correlations do not fill the e'_g hole pockets in $Na_{0.3}CoO_2$

A. Liebsch[1] and H. Ishida[2]

[1] Institut für Festkörperforschung, Forschungszentrum Jülich, 52425 Jülich, Germany
[2] College of Humanities and Sciences, Nihon University, and CREST JST, Tokyo 156, Japan

Received 26 October 2007 / Received in final form 9 January 2008
Published online 13 March 2008 –

Abstract. There exists presently considerable debate over the question whether local Coulomb interactions can explain the absence of the small e'_g Fermi surface hole pockets in photoemission studies of $Na_{0.3}CoO_2$. By comparing dynamical mean field results for different single particle Hamiltonians and exact diagonalization as well as quantum Monte Carlo treatments, we show that, for realistic values of the Coulomb energy U and Hund exchange J, the e'_g pockets can be slightly enhanced or reduced compared to band structure predictions, but they do not disappear.

PACS. 71.18.+y Fermi surface: calculations and measurements; effective mass, g factor – 71.27.+a Strongly correlated electron systems; heavy fermions – 74.70.-b Superconducting materials

1 Introduction

The Fermi surface of a material is one of its most fundamental properties. Usually, it can be understood, at least qualitatively, within density functional theory. It came as a surprise, therefore, when several angle-resolved photoemission (ARPES) studies on the intercalated layer compound $Na_{0.3}CoO_2$ [1–4] revealed a fundamentally different shape of the Fermi surface than predicted by local density approximation (LDA) band theory [5]. On the other hand, the overall width of the Co $3d$ bands in the ARPES data was found to be only moderately reduced compared to the LDA value. Essentially, the partially filled Co $3d$ t_{2g} bands should give rise to a large a_g hole pocket centered around Γ, and six small hole pockets of e'_g character along the ΓK directions of the hexagonal Brillouin Zone. These e'_g pockets have not yet been observed in ARPES experimental work. Bulk sensitive Shubnikov-de Haas data [6] reveal two frequencies, but it is not clear whether they are consistent with the LDA calculations. Recent Compton scattering measurements, however, provide evidence that the e'_g pockets do indeed exist [7]. The role of the e'_g pockets for the superconducting hydrated phase of $Na_{0.3}CoO_2$ is also a subject of intense investigations [8]. In view of the narrow width of the Co t_{2g} bands ($W \approx 1.5$ eV), one possible source of the discrepancy between ARPES and band theory might be the effect of intra-$3d$ Co Coulomb interactions which, in principle, could enhance orbital polarization by leading to a charge transfer from a_g to e'_g subbands, and, eventually, to a shift of the e'_g bands below the Fermi level.

The influence of Coulomb interactions on the Fermi surface of $Na_{0.3}CoO_2$ has been investigated by several groups, using various theoretical methods and levels of approximation [9,12–17]. Ishida et al. [9] applied dynamical mean field theory (DMFT) [10] based on the multi-orbital quantum Monte Carlo (QMC) method, together with a single-particle Hamiltonian derived from an accurate tight-binding fit of the t_{2g} bands to the linearized augmented plane wave (LAPW) band structure. The result of this work was that, for Coulomb energies $U \approx 3.0 \ldots 3.5$ eV and exchange $J = U/4$, the e'_g hole pockets were slightly enlarged compared to the LDA Fermi surface, in contrast to the ARPES data. The width of the occupied part of the t_{2g} bands, however, was found to be about 0.7 eV, in approximate agreement with ARPES measurements [1–4]. To avoid sign problems, only Ising-like exchange terms were included in the QMC calculation. It was also shown that an LDA+U [11] treatment can lead to enlarged or reduced e'_g hole pockets, depending on whether U is smaller or larger than $5J$, respectively.

At the same time, Zhou et al. [12] investigated this problem within the Gutzwiller approach in the large U, $J = 0$ limit. Using a slightly different tight-binding fit to the LDA bands, these authors found that the e'_g bands were shifted below E_F, and that the width of the t_{2g} bands was strongly reduced from 1.5 eV to about 0.5 eV. Thus, while the Fermi surface appears to agree with the ARPES data, the band narrowing is much stronger than experimentally observed. Similar Gutzwiller calculations in the $U \to \infty$, $J = 0$ limit were recently carried out by Shorikov et al. [13], with results similar to those of reference [12]. Since the Gutzwiller method replaces the frequency dependent complex self-energy by parameters providing orbital dependent energy shifts and band

narrowing, it represents an approximation to DMFT. Moreover, for $U \to \infty$, complete orbital polarization is to be expected. Thus, for a meaningful comparison with ARPES data, it is important to extend the Gutzwiller approach to realistic Coulomb and exchange energies appropriate for Co.

The influence of correlations on the electronic properties of hydrated $Na_{0.35}CoO_2$ was also investigated by Landron and Lepetit [14] within quantum chemical methods for embedded CoO_6 and Co_2O_{10} clusters. The crystal field splitting between a_g and e'_g orbitals was found to be $\Delta = 315$ meV, and the Coulomb and exchange energies $U = 4.1$ eV and $J = 0.28$ eV. At present, it is not clear how these parameters, in particular, the large value of Δ, would be modified for larger clusters that are required to describe the electronic properties of the extended system. Slave-boson mean field calculations by Bourgeois et al. [15] based on $\Delta = 315$ meV and $U \to \infty$ revealed a pure a_g Fermi surface and a t_{2g} band width of 0.5 eV, similar to the results of reference [12].

To examine the role of Hund exchange contributions not included in the QMC/DMFT, Perroni et al. [16] applied a new multi-band exact diagonalization DMFT scheme to $Na_{0.3}CoO_2$. This approach does not suffer from sign problems and includes spin-flip and pair-exchange terms. Also, larger values of U and lower temperatures can be handled than via QMC. The result of this study was that there is little difference between Hund and Ising exchange, and that, for $U = 3 \ldots 5$ eV and $J = U/4$, the e'_g pockets were slightly enlarged, in agreement with the QMC/DMFT results. Also, the band narrowing was found to be consistent with the QMC treatment and with the ARPES data.

Most recently, Marianetti et al. [17] studied the problem of the e'_g hole pockets in $Na_{0.3}CoO_2$ by applying a new continuous-time QMC/DMFT version that allows to reach larger U and lower temperatures. The single-particle Hamiltonian was the same as in reference [12], except for the crystal field splitting $\Delta = E_{a_g} - E_{e'_g}$ that shifts the a_g bands up and the e'_g bands down. For $U = 3 \ldots 5$ eV and $J = 0$, reduced e'_g pockets are found for $\Delta = -10$ meV, and fully suppressed pockets if Δ is increased to $50 \ldots 100$ meV. Their results appear to be in agreement with reference [12] and in disagreement with reference [9]. Since the DMFT calculations, however, were not done for the same input Hamiltonian and U, J values as those in references [9,16], the origin of the conflicting trends is presently unknown.

The purpose of this work is to resolve this issue and to analyze the role of the single-particle Hamiltonian $H(k)$ and Coulomb and exchange energies for the charge transfer between t_{2g} bands. In particular, we show that the ED and QMC many-body calculations are in perfect agreement if identical input parameters are employed. On the other hand, the two different versions of $H(k)$ used in references [9,16] and [12,17] (below we refer to them as H_1 and H_2, respectively) give rise to a slight, but significant difference in the variation of e'_g occupancy with U: whereas H_1 yields decreasing e'_g occupancy with increasing U, H_2 gives the opposite trend. We show that these differences are caused by the t_{2g} crystal fields Δ contained H_1 and H_2. The key point, however, is that, for realistic Coulomb and exchange energies, i.e., $U \approx 3 \ldots 5$ eV and $J \approx 0.72$ eV [18], the differences caused by $H(k)$ are small and do not affect the controversy concerning the shape of the Fermi surface. Both versions of $H(k)$ yield the result that, without an additional a_g/e'_g crystal field splitting, Coulomb interactions do not eliminate the e'_g hole pockets. The overall topology of the Fermi surface remains the same as predicted by LDA band theory.

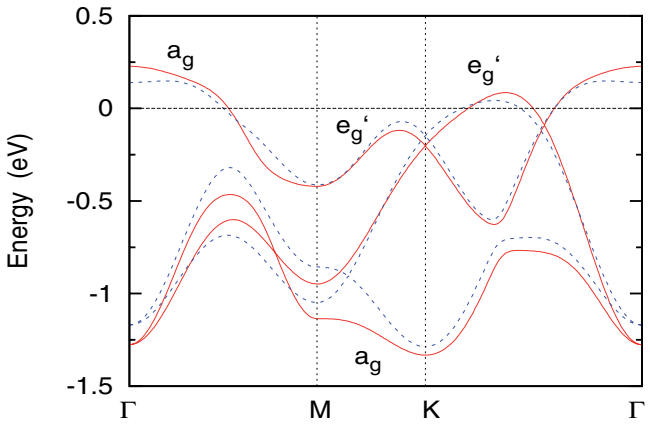

Fig. 1. Tight-binding fits to LDA t_{2g} band structure of $Na_{0.3}CoO_2$. Solid (red) curves: $H_1(k)$ used in references [9,16], dashed (blue) curves: $H_2(k)$ used in references [12,17]; $E_F = 0$.

2 Theory

Figure 1 shows the tight-binding fits to the partially occupied Co $3d$ t_{2g} bands used in references [9,16] and [12,17]. The Hamiltonian $H_1(k)$ used in references [9,16] is specified in the Appendix [19]. The one employed in reference [17] is given in reference [12]. The total occupancy is 5.3. The a_g and e'_g occupancies (per spin band) are $n_{a_g} \approx 0.80$ and $n_{e'_g} \approx 0.925$. Although both Hamiltonians give similar energy bands, they differ in a fundamental aspect: the predominant a_g wave function character of the lowest LAPW band along MK of reference [5] is correctly reproduced via H_1, resulting in a van Hove singularity in the a_g density of states near -1.12 eV, as shown in Figure 2. In contrast, the two lowest bands derived from H_2 cross along MK, so that this singularity is shifted to -0.84 eV, implying a significant narrowing of this subband. The lowest H_2 band at M has e'_g character and gives only a weak step at -1.02 eV in the density of states. Since the influence of Coulomb interactions is highly sensitive to the band width and the distribution of spectral weight within a band, and to the effective crystal field splitting between subbands, these differences should affect also the correlation induced charge transfer between t_{2g} bands.

The top of the H_2 a_g band at Γ is seen to exhibit a minimum which is absent for H_1 and leads to a pronounced peak in the density of states. This spectral weight is

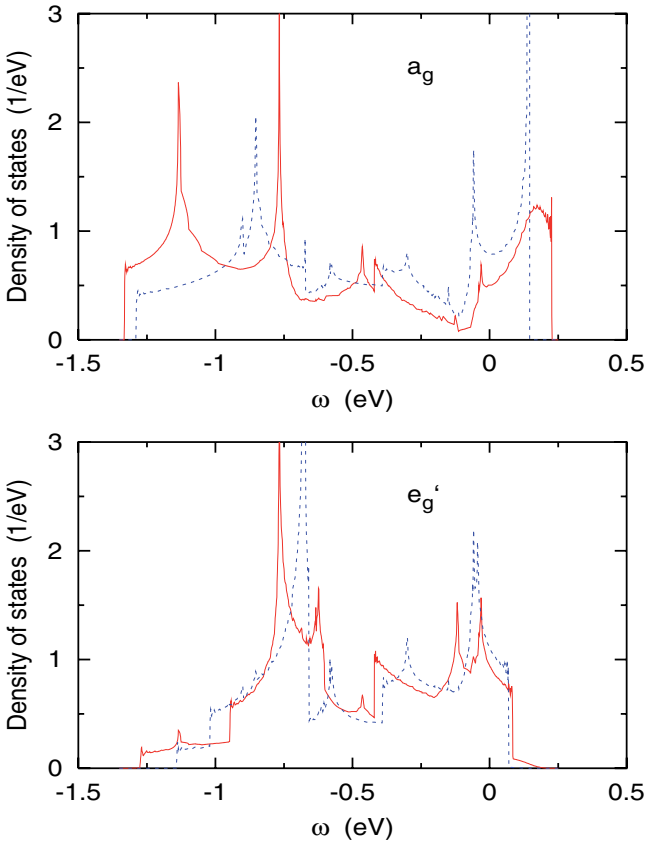

Fig. 2. Comparison of a_g and e'_g density of states. Solid (red) curves: $H_1(k)$, dashed (blue) curves: $H_2(k)$, $E_F = 0$.

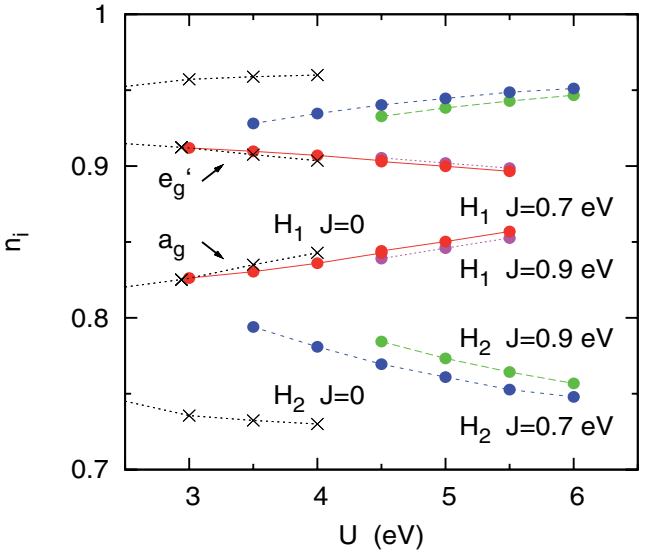

Fig. 3. Subband occupancies as a function of U for fixed J derived within ED/DMFT for $T = 20$ meV. Solid (red) curves: H_1, $J = 0.7$ eV; dotted (magenta) curves: H_1, $J = 0.9$ eV; dashed (blue) curves: H_2, $J = 0.7$ eV; long-dashed (green) curves: H_2, $J = 0.9$ eV. For comparison, some results for $J = 0$ are also shown (crosses).

distributed over a slightly wider energy range in the case of H_1. The minimum is present in the LDA LAPW band structure to which both Hamiltonians were fitted. It is caused by interplanar interactions in the double layer of the unit cell. These interactions are absent in H_1 as well as H_2. Moreover, the bulk a_g density of states does not exhibit a sharp peak in this region. Thus, the H_1 a_g density shown in Figure 2 should be more appropriate than the one derived from H_2.

Despite these differences, near E_F both Hamiltonians yield very similar bands. The e'_g band extends less than 100 meV above E_F, and both models exhibit the a_g / e'_g crossing along ΓK just below E_F. Note that this crossing exists only along ΓK. Away from this line the upper e'_g band hybridizes with the a_g band so that a rapidly increasing gap is opened up as soon as the parallel momentum deviates from ΓK.

We now discuss the correlation induced changes of the t_{2g} bands of $Na_{0.3}CoO_2$ obtained within DMFT. We had previously shown that, for Hamiltonian H_1, the QMC and ED results of references [9,16] for Ising exchange are in excellent agreement and that both schemes yield reduced orbital polarization with increasing U. Moreover, this trend was found to be insensitive to the choice of J, with virtually no difference between anisotropic Ising and isotropic Hund exchange within ED.

We have applied the ED approach of reference [16] to H_2 to check its consistency with the QMC formalism used in reference [17]. For $U = 3$ eV, $J = 0$, $\Delta = -10$ meV the subband self-energies as a function of Matsubara frequency were found to be in almost quantitative agreement. In view of the inevitable slight numerical differences between these DMFT approaches, the excellent agreement of the ED and QMC results is indeed remarkable. We also point out that both DMFT schemes take proper account of static and dynamical correlations.

The unexpected result of this calculation is that, with H_2 as input, both ED and QMC schemes yield *enhanced* orbital polarization: for $U = 3$ eV, $J = 0$, the subband occupancies are $n_{a_g} = 0.735$, $n_{e'_g} = 0.957$, compared to the LDA values $n_{a_g} = 0.8$, $n_{e'_g} = 0.925$. This charge transfer is opposite to the *reduced* orbital polarization obtained for H_1: $n_{a_g} = 0.825$, $n_{e'_g} = 0.91$.

Figure 3 shows that similar systematic differences between H_1 and H_2 are found at other values of U, J. To eliminate other sources of possible differences, all results are derived using the ED/DMFT approach [16] at $T = 20$ meV. Regardless of the choice of J, H_1 leads to a reduction of $n_{e'_g}$ as a function of U, whereas H_2 yields increasing $n_{e'_g}$. As in the case of H_1, Hund and Ising exchange give nearly identical results for H_2. Thus, although the single-particle band structure and density of states derived from H_1 and H_2 look qualitatively similar, these two Hamiltonians lead to a small, but significant difference in the variation of the subband occupancies with Coulomb energy.

To analyze the origin of this unusual behavior we simplify the evaluation of the quasi-particle Green's function

$$G(i\omega_n) = \sum_k [i\omega_n + \mu - H(k) - \Sigma(i\omega_n)]^{-1}, \quad (1)$$

where $\omega_n = (2n+1)\pi/\beta$ are Matsubara frequencies, with $\beta = 1/k_B T$ and temperature T. G, H and Σ are (3×3) matrices in the t_{2g} basis. Because of the planar hexagonal symmetry, the diagonal elements of G are identical, and so are the off-diagonal elements. The same applies to Σ. In the a_g, e'_g basis, these quantities become diagonal, with elements $G_{a_g} = G_{11} + 2G_{12}$ and $G_{e'_g} = G_{11} - G_{12}$, and analogous expressions for Σ_{a_g,e'_g}. In this basis, the Green's functions can be approximately written as

$$G_i(i\omega_n) = \int d\omega \rho_i(\omega)[i\omega_n + \mu - \omega - \Sigma_i(i\omega_n)]^{-1}, \quad (2)$$

where $\rho_i(\omega)$ are the a_g and e'_g density of states components shown in Figure 2. We have checked that equation (2) yields DMFT solutions with the same trend as the ones derived from equation (1). Thus, the different solutions obtained for H_1 and H_2 are directly related to the different shapes of the respective density of states distributions. As is evident from Figure 2, the e'_g densities are quite similar for both Hamiltonians. Indeed, replacing one by the other does not alter the trends for the charge transfer shown in Figure 3. It is clear, therefore, that the different shapes of the a_g density of states are the source of the opposite orbital polarization found for H_1 and H_2.

As pointed out above, the fact that the lowest H_2 bands cross along MK leads to an upward shift of the lowest a_g van Hove singularity by about 0.3 eV. One can simulate this redistribution of spectral weight by reducing the a_g density of H_1 in the range $\omega < -0.7$ eV and amplifying it in the region $-0.7\,\text{eV} < \omega < 0$, such that the occupied weight remains 0.8. This deformation is sufficient to reverse the trend of $n_i(U)$ and give rise to a weak enhancement of orbital polarization.

Evidently, the upward shift of spectral weight caused by the band crossing along MK implies a relative shift of $3d$ energy levels. In the case of H_1, the centroids of the a_g and e'_g density of states are $E_{a_g} = -0.622$ eV and $E_{e'_g} = -0.489$ eV, where $\Delta = E_{a_g} - E_{e'_g} = -133$ meV is the t_{2g} crystal field splitting. In the tight-binding fit, Δ was varied along with the hopping parameters, in order to achieve the optimum representation of the LAPW bands throughout the Brillouin Zone [9]. Clearly, its value reflects the electronic structure of the extended system. The physical origin of the negative t_{2g} crystal field, i.e., the relation $E_{a_g} < E_{e'_g}$, can be attributed to the fact that the Na^+ Coulomb field acts more strongly on the a_g orbital, which is oriented normal to the Co planes, than on the more planar e'_g orbitals. In the case of H_2, the splitting was chosen as $\Delta = -10$ meV, and only the hopping parameters were fitted [12]. The a_g and e'_g centroids therefore nearly coincide: $E_{a_g} = -0.489$ eV and $E_{e'_g} = -0.479$ eV. Note that, in both cases, $E_{a_g} < E_{e'_g}$ despite $n_{a_g} < n_{e'_g}$.

As a result of these different level splittings, correlations lead to an intriguing reversal of interorbital charge transfer: for H_1 with $\Delta = -133$ meV, the large a_g/e'_g splitting is enhanced and gives rise to a gradual filling of the a_g band with increasing U. Since, at small U, the a_g occupancy is lower than the e'_g occupancy, this charge transfer amounts to an initial reduction of orbital polarization. (At larger U, n_{a_g} might become larger than $n_{e'_g}$, so that the same correlation induced $e'_g \rightarrow a_g$ charge transfer eventually could turn into enhanced orbital polarization.) In contrast, the small crystal field included in H_2, $\Delta = -10$ meV, is too weak to enforce a correlation induced downward shift of the a_g band. Thus, the charge transfer is dominated by the larger e'_g occupancy, giving enhanced orbital polarization even at small U.

According to the above discussion several arguments reveal that the tight-binding fit obtained from Hamiltonian $H_1(k)$ is more appropriate than the one derived from $H_2(k)$: (i) the important crystal field parameter is included in the fit, rather than chosen independently; (ii) $H_1(k)$ reproduces the crossing of the low-lying bands along MK whereas $H_2(k)$ does not, giving rise to a spurious upward shift of a_g spectral weight and, because of charge conservation, a downward shift of the e'_g bands; (iii) the better fit derived from $H_2(k)$ at the top of the a_g band is artificial because the LDA bands include interplanar interaction that the tight-binding model does not; reproduction of features that stem from this interaction is actually undesirable.

Thus, since $H_1(k)$ provides the more accurate fit to the LAPW bands, the correlation induced reduction of orbital polarization in the range of reasonable values of U and J should be more realistic than the opposite trend obtained for $H_2(k)$. As argued in references [9,16], therefore, local Coulomb correlations should slightly enhance the e'_g hole pockets of $Na_{0.3}CoO_2$.

The important point which we like to emphasize, however, is that, even if $H_2(k)$ is used as input in the many-body DMFT calculation, the reversal of charge transfer relative to the one found for $H_1(k)$ is not large enough to push the e'_g bands fully below E_F.

This is illustrated in Figure 4 which shows the dispersion of the quasi-particle bands for Hamiltonian H_2 at $U = 4.0$ eV, $J = 0.7$ eV. This band structure was generated by transforming the subband self-energies $\Sigma_i(i\omega_n)$ derived within ED/DMFT to real frequencies by using the procedure discussed in reference [16]. The e'_g Fermi surface pockets are associated with the flat bands extending slightly above E_F along ΓK. The occupied part of the bands is about 0.7 eV wide, in qualitative agreement with the photoemission data. For larger U the e'_g hole pockets become smaller and might even disappear, but the overall width of the t_{2g} bands then also decreases and becomes smaller than observed experimentally.

According to Figure 3, the correlation induced interorbital charge transfer in the case of H_2 is more sensitive to the choice of the Hund's exchange J than in the case of H_1, in particular, for $J = 0$. This surprising qualitative difference between the two tight-binding Hamiltonians is currently under investigation and will be addressed in future work.

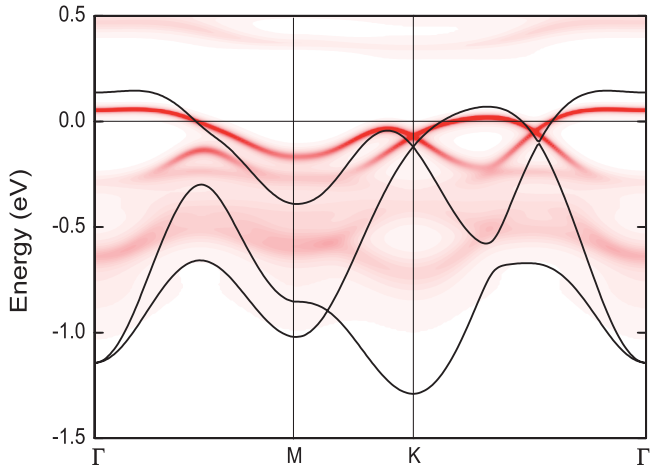

Fig. 4. (Color online) Broadened (red) distributions: dispersion of quasi-particle bands of $Na_{0.3}CoO_2$ calculated within ED/DMFT for Hamiltonian $H_2(k)$ (reference [12]) at $T = 20$ meV, $U = 4.0$ eV, $J = 0.7$ eV. Solid (black) curves: corresponding LDA bands.

3 Discussion

As pointed out above, the a_g band crosses the upper branch of the e'_g approximately half-way between Γ and K. Away from this symmetry direction, both bands may interact so that a hybridization gap opens up. Moreover, the e'_g band rapidly disperses downwards away from the ΓK direction and shifts below E_F. Because of the finite aperture of the electron detector in angle resolved photoemission, the data necessarily integrate over a small window in $k_\parallel$. Since the ΓK line represents only a single point within this window, the main part of detected emission spectrum must therefore exhibit a gapped dispersion below the maximum of the e'_g band, i.e., close to or below E_F.

We also note that, because of the orbital character of these bands (the a_g orbital points away from the plane of Co atoms, while the e'_g orbitals lie mainly within the Co plane) the emission from the a_g band tends to be much stronger than from the e'_g bands [23]. A clear distinction between these bands is therefore nontrivial. It would therefore be valuable to perform ARPES measurements for s-polarized and p-polarized light in order to exploit elementary selection rules to distinguish bands whose wavefunctions are odd or even with respect to reflections about the plane defined by a specific $\boldsymbol{k}_\parallel$ (determined by the detector azimuthal orientation) and the surface normal. Such measurements were in fact carried out by Qian et al. [3] and are in good correspondence with the expected odd/even band character along ΓM. Surprisingly, however, along ΓK s-polarization was found to yield nearly the same band dispersion as p-polarization despite the different symmetry properties of the t_{2g} bands (see Figs. 4c and 4d of Ref. [3]). Also, according to the uncorrelated and correlated band structures shown in Figures 1 and 4, at K the a_g band must lie far below the degenerate e'_g bands, which is not evident from the ARPES data [2,3].

As discussed in reference [17], for $J = 0$ a positive crystal field $\Delta \approx 50 \ldots 100$ meV enhances the orbital polarization, so that, in combination with local Coulomb interactions, the e'_g hole pockets disappear. Since for realistic exchange energies $J = 0.7 \ldots 0.9$ eV the overall effect of Coulomb correlations is weaker, Δ should be accordingly larger [20]. If we assume the ARPES data to be correct, the crucial question then concerns the physical origin of such a crystal field. Evidently, it is not related to on-site Coulomb interactions in the spirit of a single-site DMFT. Non-local effects stemming from the momentum dependence of the self-energy have not yet been explored and could be studied by using a cluster extension of the DMFT. Na disorder was shown to eliminate the pockets at large Na concentrations near $x = 0.7$ [21,22], but is believed to be too weak to have a significant effect on the Fermi surface near $x = 0.3$. Surface effects which have played an important role in ARPES data on other perovskites, such as $Ca_{2-x}Sr_xRuO_4$ and $Ca_{1-x}Sr_xVO_3$, should also be investigated, in particular, the effect of Na induced states on the first layer. Moreover, possible structural distortions, such as intra-planar buckling, and their connection to the opening of the a_g/e'_g hybridization gap along ΓK should be explored.

We finally mention that, as emphasized in reference [17], the e'_g hole pockets are also important for the understanding of the heat capacity of $Na_{0.3}CoO_2$. At present, the experimental value, $\gamma \approx 12 \ldots 16$ mJ/mol Co K^2, is difficult to reconcile with the LDA result, $\sim$14 mJ/mol Co K^2, and an effective mass enhancement of about 2, as derived within DMFT. For a detailed analysis of this quantity it might be necessary to relax the pinning condition for the total density of states implied by the single-site approximation and allow for non-local effects.

4 Conclusion

In summary, we have presented a detailed discussion of single-particle and many-body correlation effects that influence the inter-orbital charge transfer among t_{2g} conduction bands and the shape of the Fermi surface of $Na_{0.3}CoO_2$. The results reveal that slight differences among the tight-binding Hamiltonians lead to increasing or decreasing orbital polarization. This reversal of subband occupancies as a function of U underlines the importance of using a high-quality single-particle basis as input in the many-body calculation. On the other hand, by comparing results obtained from ED and QMC impurity treatments for identical input Hamiltonians, we have found excellent agreement, confirming the reliability of these complementary DMFT approaches. These calculations resolve the puzzling apparent discrepancies between DMFT results reported in references [9,16] and [17] for the correlation induced a_g/e'_g charge transfer in $Na_{0.3}CoO_2$.

In spite of the opposite trends found for two different tight-binding Hamiltonians, in the range of realistic Coulomb and exchange energies, the differences concerning the subband occupations are not large enough to fill

the e'_g hole pockets. The main result of this work is therefore that, unless additional structural modifications enhance the intrinsic t_{2g} crystal field and shift the e'_g bands below E_F, the topology of the Fermi surface of $Na_{0.3}CoO_2$ remains the same as predicted by LDA band theory.

We hope that these results encourage further experimental and theoretical work to study in more detail the geometrical and electronic structure of this fascinating material.

One of us (A.L.) likes to thank Chris Marianetti for extensive correspondence and for sending his QMC self-energy results, and Michelle Johannes and Igor Mazin for very useful discussions. We are grateful to the authors of reference [19] for the permission to quote the matrix elements of Hamiltonian $H_1(k)$.

Appendix

In this Appendix we specify the matrix elements of Hamiltonion $H_1(k)$. The tight-binding parameters were derived using a Wannier representation of full-potential NMTO calculations using the technique described in reference [24]. The obtained parameters were subsequently adjusted to reproduce the full-potential LAPW bandstructure throughout the Brillouin Zone using a least squares fit routine. Further details will be provided in reference [19]. This tight-binding Hamiltonian is precisely the same as that used in reference [17], though the parameter set is different and therefore yields slighty different band dispersions as shown in Figure 1.

For convenience, we use a cubic coordinate system in which the unit vectors along the x, y, z axes define the hexagonal plane of Co sites. We specify $H_1(k)$ in terms of $t_{2g} = d_{xy,xz,yz}$ orbitals in this coordinate system and later transform local quantities such as the density of states to the a_g, e'_g basis via the transformation $a_g = (xy + xz + yz)/\sqrt{3}$, $e'_{g1} = (xz - yz)/\sqrt{2}$, $e'_{g2} = (2xy - xz - yz)/\sqrt{6}$. Let us define $\boldsymbol{a} = (1, -1, 0)/\sqrt{2}$ and $\boldsymbol{b} = (1, 1, -2)/\sqrt{6}$. The lines ΓM and ΓK in the two-dimensional hexagonal Brillouin zone are then given by $\boldsymbol{k} = 0 \ldots \boldsymbol{b}/2$ and $\boldsymbol{k} = 0 \ldots (\boldsymbol{b} + \boldsymbol{a}/\sqrt{3})/2$, respectively.

We introduce the cosine functions of the first three neighbor shells as

$$\begin{aligned}
cos_1 &= \cos(k'_x - k'_y)\\
cos_2 &= \cos(k'_z - k'_y)\\
cos_3 &= \cos(k'_z - k'_x)\\
cos_4 &= \cos(k'_x - 2k'_y + k'_z)\\
cos_5 &= \cos(k'_x - 2k'_z + k'_y)\\
cos_6 &= \cos(k'_y - 2k'_x + k'_z)\\
cos_7 &= \cos(2k'_x - 2k'_y)\\
cos_8 &= \cos(2k'_z - 2k'_y)\\
cos_9 &= \cos(2k'_z - 2k'_x)
\end{aligned}$$

with $k'_i = 2\pi k_i \sqrt{2/3}$.

The first-neighbor contributions to $H_1(k)$ are given by:

$$\begin{aligned}
a(1,1) &= a_1 cos_1 + a_2(cos_2 + cos_3)\\
a(2,2) &= a_1 cos_2 + a_2(cos_1 + cos_3)\\
a(3,3) &= a_1 cos_3 + a_2(cos_1 + cos_2)\\
a(1,2) &= a_3 cos_3\\
a(1,3) &= a_3 cos_2\\
a(2,3) &= a_3 cos_1
\end{aligned}$$

where

$$\begin{aligned}
a_1 &= 1.5t_{1\sigma} + 0.5t_{1\delta}\\
a_2 &= t_{1\pi} + t_{1\delta}\\
a_3 &= t_{1\delta} - t_{1\pi}.
\end{aligned}$$

The second-neighbor contributions are:

$$\begin{aligned}
b(1,1) &= b_1(cos_4 + cos_6) + b_2 cos_5\\
b(2,2) &= b_1(cos_4 + cos_5) + b_2 cos_6\\
b(3,3) &= b_1(cos_5 + cos_6) + b_2 cos_4\\
b(1,2) &= b_4(cos_5 + cos_6) + b_3 cos_4\\
b(1,3) &= b_4(cos_4 + cos_5) + b_3 cos_6\\
b(2,3) &= b_4(cos_4 + cos_6) + b_3 cos_5
\end{aligned}$$

where

$$\begin{aligned}
b_1 &= (6t_{2\sigma} + 7t_{2\pi} + 5t_{2\delta})/9\\
b_2 &= (3t_{2\sigma} + 8t_{2\pi} + 25t_{2\delta})/18\\
b_3 &= (6t_{2\sigma} - 5t_{2\pi} - t_{2\delta})/9\\
b_4 &= (-3t_{2\sigma} - 2t_{2\pi} + 5t_{2\delta})/9.
\end{aligned}$$

The third-neighbor contributions are:

$$\begin{aligned}
c(1,1) &= c_1 cos_7 + c_2(cos_8 + cos_9)\\
c(2,2) &= c_1 cos_8 + c_2(cos_7 + cos_9)\\
c(3,3) &= c_1 cos_9 + c_2(cos_7 + cos_8)\\
c(1,2) &= c_3 cos_9\\
c(1,3) &= c_3 cos_8\\
c(2,3) &= c_3 cos_7
\end{aligned}$$

where

$$\begin{aligned}
c_1 &= 1.5t_{3\sigma} + 0.5t_{3\delta}\\
c_2 &= t_{3\pi} + t_{3\delta}\\
c_3 &= t_{3\delta} - t_{3\pi}.
\end{aligned}$$

The above matrix elements correspond to a perfect octahedral symmetry. In the real lattice, however, the oxygen octahedra are slightly compressed along the z-axis of the hexagonal crystal. As a result of this non-cubic distortion the t_{2g} orbitals hybridize along directions that would normally be forbidden. To account for these interactions additional matrix elements are allowed. The complete Hamiltonian matrix is then given by

$$\begin{aligned}
H(i,j) = \epsilon_0\delta_{ij} &+ a(i,j) + b(i,j) + c(i,j) + f_0\\
&+ f_1(cos_1 + cos_2 + cos_3)\\
&+ f_2(cos_4 + cos_5 + cos_6)\\
&+ f_3(cos_7 + cos_8 + cos_9)
\end{aligned}$$

where the coefficients f_i account for non-cubic distortions. The detailed derivation of this Hamiltonian matrix will be given elsewhere [19]. The values of the hopping parameters $t_{i\alpha}$ $(i = 1 \ldots 3,\ \alpha = \sigma, \pi, \delta)$ and of the coefficients f_i $(i = 0 \ldots 3)$ which are derived from a fit to the LAPW band structure, are as follows (all in eV):

$$
\begin{aligned}
&t_{1\sigma} = 0.0432, \quad t_{1\pi} = -0.1380, \quad t_{1\delta} = 0.0202,\\
&t_{2\sigma} = -0.1228, \quad t_{2\pi} = 0.0094, \quad t_{2\delta} = 0.0570,\\
&t_{3\sigma} = -0.1322, \quad t_{3\pi} = -0.0489, \quad t_{3\delta} = -0.0347,\\
&f_1 = 0.1054, \quad f_2 = -0.0292, \quad f_3 = 0.0322.
\end{aligned}
$$

The constant off-diagonal element f_0 responsible for the t_{2g} crystal field splitting $\Delta = 3f_0$ between a_g and e'_g bands is $f_0 = -0.04424$ eV. Finally, the mean energy level $\epsilon_0 = -0.4893$ eV is adjusted so that up to the Fermi energy $E_F = 0$ there are 5.3 electrons within the t_{2g} bands. From the above definitions it follows that the centroid of the a_g band is given by $E_{a_g} = \epsilon_0 + 3f_0 = -0.622$ eV, while the e'_g centroid coincides with ϵ_0.

References

1. M.Z. Hasan et al., Phys. Rev. Lett. **92**, 246402 (2004)
2. H.-B. Yang et al., Phys. Rev. Lett. **92**, 246403 (2004); H.-B. Yang et al., Phys. Rev. Lett. **95**, 146401 (2005); H.-B. Yang et al., J. Phys. Cond. Mat. **19**, 255004 (2007)
3. D. Qian et al., Phys. Rev. Lett. **97**, 186405 (2006)
4. T. Shimojima et al., Phys. Rev. Lett. **97**, 267003 (2006)
5. D.J. Singh, Phys. Rev. B **61**, 13397 (2000)
6. L. Balicas et al., Phys. Rev. Lett. **97**, 126401 (2006)
7. J. Laverock et al., Phys. Rev. B **76**, 052509 (2007)
8. K. Kuroki, Y. Tanaka, R. Arita, Phys. Rev. Lett. **93**, 077001 (2004); M.D. Johannes, I.I. Mazin, D.J. Singh, D.A. Papaconstantopoulos, Phys. Rev. Lett. **93**, 097005 (2004); M. Mochizuki, M. Ogata, e-print [arXiv:cond-mat/0609443]; K. Kuroki et al., e-print [arXiv:cond-mat/0610494]
9. H. Ishida, M.D. Johannes, A. Liebsch, Phys. Rev. Lett. **94**, 196401 (2005)
10. For a review, see: A. Georges, G. Kotliar, W. Krauth, M.J. Rozenberg, Rev. Mod. Phys. **68**, 13 (1996)
11. A.I. Liechtenstein, V.I. Anisimov, J. Zaanen, Phys. Rev. B **52**, R5467 (1995)
12. S. Zhou, M. Gao, H. Ding, P.A. Lee, Z.Q. Wang, Phys. Rev. Lett. **94**, 206401 (2005)
13. A.O. Shorikov, V.I. Anisimov, M.M. Korshunov, e-print [arXiv:cond-mat/0705.1408]
14. S. Landron, M.B. Lepetit, Phys. Rev. B **74**, 18450785 (2006)
15. A. Bourgeois, A.A. Aligia, T. Kroll, M.D. Núñez-Regueiro, Phys. Rev. B **75**, 174518 (2007)
16. C.A. Perroni, H. Ishida, A. Liebsch, Phys. Rev. B **75**, 045125 (2007)
17. C.A. Marianetti, K. Haule, O. Parkollet, Phys. Rev. Lett. **99**, 246404 (2007)
18. T. Kroll, A.A. Aligia, G.A. Sawatzky, Phys. Rev. B **74**, 115124 (2006)
19. O.K. Andersen, I.I. Mazin, O. Jepson, M.D. Johannes, to be published
20. For large Δ it might be necessary to readjust the hopping parameters to describe the electronic properties of the system
21. D.J. Singh, D. Kasinathan, Phys. Rev. Lett. **97**, 016404 (2006)
22. C.A. Marianetti, G. Kotliar, G. Ceder, Phys. Rev. Lett. **92**, 196405 (2002)
23. M.D. Johannes (unpublished). In this context it is worthwhile to recall that truly intraplanar orbitals (i.e. d_{xy} and $d_{x^2-y^2}$) have $m = \pm 2$ quantum number and therefore give vanishing emission along the surface normal since the outgoing electron then has $m = 0$ and the photon provides only $\Delta m = \pm 1$
24. O.K. Andersen, T. Saha-Dasgupta, Phys. Rev. B **62**, 16219(R) (2000); O.K. Andersen, T. Saha-Dasgupta, S. Ezhov, Bull. Mater. Sci. **26**, 19 (2003)